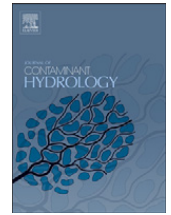




Contents lists available at ScienceDirect

## Journal of Contaminant Hydrology

journal homepage: [www.elsevier.com/locate/jconhyd](http://www.elsevier.com/locate/jconhyd)

## Examining the influence of heterogeneous porosity fields on conservative solute transport

Bill X. Hu<sup>a,\*</sup>, Mark M. Meerschaert<sup>b</sup>, Warren Barrash<sup>c</sup>, David W. Hyndman<sup>d</sup>, Changming He<sup>e</sup>, Xinya Li<sup>a</sup>, Luanjing Guo<sup>a</sup><sup>a</sup> Department of Geological Sciences, Florida State University, Tallahassee, FL 32306, United States<sup>b</sup> Department of Statistics and Probability, Michigan State University, East Lansing, MI 48824, United States<sup>c</sup> CGISS, Department of Geosciences, Boise State University, Boise, ID 83725, United States<sup>d</sup> Department of Geological Sciences, Michigan State University, East Lansing, MI, 48824, United States<sup>e</sup> Delaware Geological Survey, University of Delaware, Newark, DE 19716, United States

## ARTICLE INFO

## Article history:

Received 23 February 2009

Received in revised form 5 June 2009

Accepted 11 June 2009

Available online 27 June 2009

## Keywords:

Heterogeneity

Porosity

Hydraulic conductivity

Geostatistics

Fractal

Solute transport

## ABSTRACT

It is widely recognized that groundwater flow and solute transport in natural media are largely controlled by heterogeneities. In the last three decades, many studies have examined the effects of heterogeneous hydraulic conductivity fields on flow and transport processes, but there has been much less attention to the influence of heterogeneous porosity fields. In this study, we use porosity and particle size measurements from boreholes at the Boise Hydrogeophysical Research Site (BHRS) to evaluate the importance of characterizing the spatial structure of porosity and grain size data for solute transport modeling. Then we develop synthetic hydraulic conductivity fields based on relatively simple measurements of porosity from borehole logs and grain size distributions from core samples to examine and compare the characteristics of tracer transport through these fields with and without inclusion of porosity heterogeneity. In particular, we develop horizontal 2D realizations based on data from one of the less heterogeneous units at the BHRS to examine effects where spatial variations in hydraulic parameters are not large. The results indicate that the distributions of porosity and the derived hydraulic conductivity in the study unit resemble fractal normal and lognormal fields respectively. We numerically simulate solute transport in stochastic fields and find that spatial variations in porosity have significant effects on the spread of an injected tracer plume including a significant delay in simulated tracer concentration histories.

Published by Elsevier B.V.

### 1. Introduction

It is well known that heterogeneity in natural porous formations controls groundwater flow and solute transport. Well-controlled field-scale tracer tests and transport experiments indicate that knowledge of heterogeneity is generally required to predict solute transport (e.g., Mackay et al., 1986; Guven et al., 1992; Mas-Pla et al., 1992; Kapoor and Gelhar, 1994; Phanikumar et al., 2005; Salamon et al., 2007). In the last three decades, many theoretical and experimental studies have been conducted to characterize the heterogeneous distributions of

hydraulic and chemical parameter distributions in natural formations and to investigate the effects of heterogeneities on flow and transport processes (e.g., Dagan, 1989; Gelhar, 1993; Cushman, 1997; Hyndman et al., 2000; Zhang, 2002; Rubin, 2003; Meerschaert et al., 2006). However, the complexity of most natural formations coupled with limited available data has posed challenges for accurate modeling of flow and transport in heterogeneous systems. Natural formations often exhibit multi-scale or hierarchical heterogeneities (e.g., Gelhar et al., 1992; Barrash and Clemo, 2002; Molz et al., 2004; Neuman et al., 2008); the appropriate way to characterize the spatial distributions of parameters in such formations and evaluate the significance of heterogeneities at various scales on flow and transport are unresolved issues.

\* Corresponding author. Tel.: +1 850 644 3743.

E-mail address: [hu@gly.fsu.edu](mailto:hu@gly.fsu.edu) (B.X. Hu).

A common assumption is that the physical heterogeneity of aquifers needed to explain groundwater flow and transport is manifested entirely in the hydraulic conductivity field, and that variations in porosity have negligible effects except as a contributor to hydraulic conductivity heterogeneities. Hydraulic conductivity commonly varies by three to four orders of magnitude within short distances, while porosity generally ranges between 0.1 and 0.55 in unconsolidated granular aquifers (e.g., Freeze and Cherry, 1979; Atkins and McBride, 1992). In aquifers with distinct facies or zones, porosity is generally assumed to be constant while hydraulic conductivity is treated, from simple to complex, as (1) a constant in each zone; (2) a stationary variable within each zone; or occasionally (3) a spatial random variable with fractal structure in the whole study domain.

Although the correlation between hydraulic conductivity and porosity has been studied for several decades (e.g., Fraser, 1935; Archie, 1950), most efforts have used this correlation to predict conductivity values from porosity measurements in cemented rock environments (Nelson, 1994; Lahm et al., 1995). In unconsolidated aquifers, hydraulic conductivity is generally assumed to be positively correlated with porosity, but to achieve reasonable correlations it is important to incorporate information about the grain size distribution as proxies for the pore size distribution (e.g., see discussion of Kozeny–Carman theory in Panda and Lake, 1994; Charbeneau, 2000) and perhaps the facies (e.g., Pryor, 1973). That is, porosity is simply the fractional pore volume in the formation, while hydraulic conductivity depends more on pore sizes and their connectivity.

Unfortunately, the correlation between hydraulic conductivity and porosity is partial and nonlinear. There have been few studies of the effect of the spatial variability of porosity on flow and transport. Based on a synthetic case and an assumed spatial correlation between the two parameters, Hassan et al. (1998) and Hassan (2001) concluded that porosity variations will significantly influence solute transport. Based on field experimentation at the Lauswiesen site, Riva et al. (2006) estimated hydraulic conductivity values based on particle size and hydraulic test data. They then studied the influence of these conductivity heterogeneities on solute transport, however, the effective porosity was assumed to be a constant. Later, they extended their study by considering both hydraulic conductivity and porosity to be random variables, but the log conductivity was linearly correlated with log porosity, and the particle size contribution to conductivity was not considered (Riva et al., 2008).

In this study, we examine the effects of spatial variations of porosity on both the likely hydraulic conductivity distribution and conservative solute transport. We investigate transport behavior for synthetic aquifers based on porosity and grain size data from the unconsolidated sedimentary aquifer at the Boise Hydrogeophysical Research Site (BHRS). 2D synthetic hydraulic conductivity and porosity fields are generated based on information from one of the hydrostratigraphic units at the site, Unit 3, which has relatively mild heterogeneity (Barrash and Clemo, 2002; Barrash and Reboulet, 2004). In this way, we can evaluate the significance of including porosity in the analysis of conservative solute transport for such a mildly heterogeneous aquifer case where effects may be easier to assess than in highly heterogeneous systems.

We use data from the BHRS field site to investigate methods to geostatistically characterize the porosity distributions with limited data in a hydrostratigraphic unit, and how porosity and particle size data can be used to develop plausible hydraulic conductivity fields. We then examine how porosity variations affect solute transport and use Monte Carlo methods to investigate the combined effects of porosity and conductivity heterogeneities on transport.

## 2. Field site

The Boise Hydrogeophysical Research Site (BHRS) is located on a gravel bar adjacent to the Boise River near Boise, Idaho (Fig. 1) and was established to develop and test minimally-invasive methods to quantitatively characterize subsurface heterogeneities (Barrash et al., 1999; Clement et al., 1999). Eighteen wells at the site were cored through 18–21 m of unconsolidated, coarse (cobble and sand) fluvial deposits and were completed into the underlying clay. All wells are constructed with 10-cm-ID PVC and are fully screened through the unconfined fluvial aquifer. Of the 18 wells, 13 are concentrated in the 20-m-diameter central area of the BHRS, and the remaining five (X-wells) are “boundary” wells (Fig. 1).

In the central area of the site (Fig. 2), the unconfined aquifer is composed of a sequence of cobble-dominated sediment packages (Units 1–4) overlain by a channel sand (Unit 5) that thickens toward the Boise River and pinches out in the center of the well field (Barrash and Clemo, 2002; Barrash and Reboulet, 2004). The aquifer is underlain by a red clay layer across the site. Units 1 and 3 have relatively low porosities (means of 0.18 and 0.17, respectively) with low variance (0.00050 and 0.00059, respectively), while Units 2 and 4 have higher porosities (means of 0.24 and 0.23, respectively) and higher variance (0.00142 and 0.00251, respectively). In particular, Unit 4 includes lenses that are smaller-scale subunits (i.e., bodies with distinct parameter populations).

Porosity logs have been used to evaluate both the stratigraphy and representative geostatistical structure of aquifer materials at the site (Barrash and Clemo, 2002; Barrash and Reboulet, 2004). These logs were constructed using neutron log measurements taken at 0.06 m intervals below the water table in all wells at the BHRS. The estimated region of influence of the logging tool is a somewhat spherical volume with radius of approximately 0.2 m (Keys, 1990). The neutron logs are repeatable: four runs in well C5 had pair-wise correlation coefficients ranging from 0.935 to 0.966 (Barrash and Clemo, 2002). Conversion of neutron counts to porosity values in water-filled boreholes is well established (Hearst and Nelson, 1985; Rider, 1996) with a petrophysical transform using high and low end-member counts associated with low and high porosity values, respectively. End-member estimates can be made from values for similar deposits such as high porosity clean fluvial sands (~0.50 – e.g., see Pettyjohn et al., 1973; Atkins and McBride, 1992) and low porosity conglomerate with cobble framework and sandy matrix (~0.12 – e.g., see Jussel et al., 1994; Heinz et al., 2003). Working from well-constrained end-member porosity values, we estimate the uncertainty at the high end of the scale (in sand) to be  $\pm 5\%$  and at the low end to be  $\pm 10\%$  of the measured porosity percentages. Considering the nature of the transform and recognizing the high degree of repeatability of the logs, we

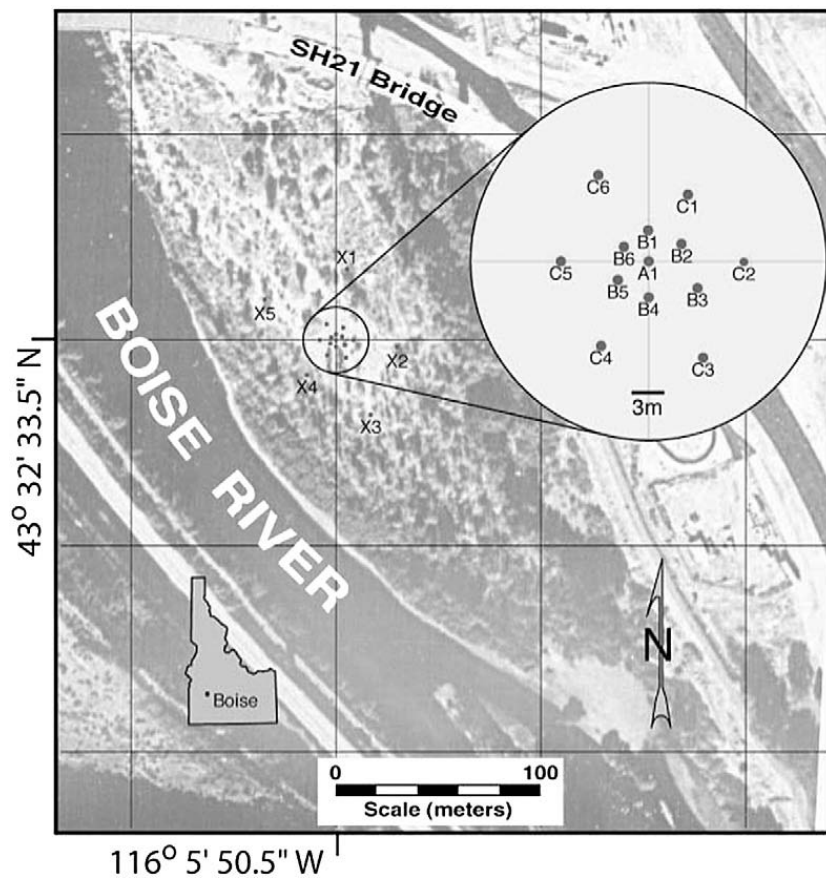


Fig. 1. Air photo of the BRHS with a map of the wells near the Boise River.

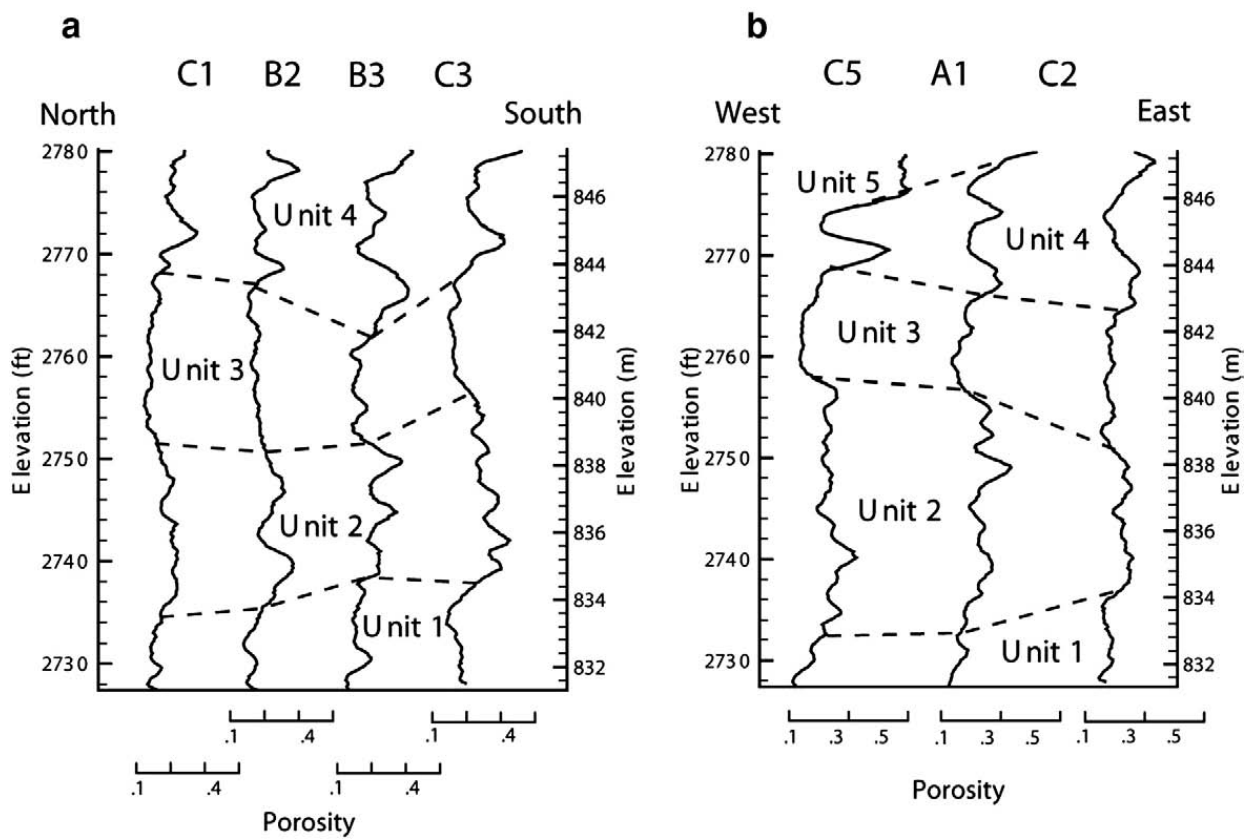


Fig. 2. Cross-sections of porosity logs showing hydrostratigraphy at the BHRS (see Fig. 1 after Barrash and Clemo, 2002).

can expect that rank consistency of relative porosity values is maintained to the measurement noise level.

Hydraulic conductivity values were estimated for the BHRS using porosity data from logs and grain size distribution data from core samples ranging in length from 0.075 to 0.3 m (Reboulet and Barrash, 2003; Barrash and Reboulet, 2004) and a modified form of the Kozeny–Carman equation (Clarke, 1979; Heinz et al., 2003; Hughes, 2005). The modified equation is based on the understanding that, for the cobble-dominated portions of the aquifer at the BHRS (i.e., Units 1 and 3, and most of Units 2 and 4), groundwater flow occurs through the pores of a sand-to-fine gravel (0.0625–9.525 mm) “matrix” that exists within the interstices of “framework” cobbles. For this system of pores ( $n$  = total porosity), framework cobble fraction ( $V_c$ ), and matrix fraction ( $V_m$ ), where  $n + V_c + V_m = 1.0$ , the framework cobbles can be considered a fraction of the flow cross-section (equal to the fraction of sample volume) that is blocking flow. The sample porosity (linear average of porosity log measurements across a given core sample) is adjusted to be assigned totally to the matrix. The adjusted porosity  $\phi = n / (n + V_m)$  is used in the Kozeny–Carman equation to calculate a conductivity value for the matrix portion of the aquifer. The resulting matrix conductivity value is then multiplied by  $(n + V_m)$  to recover a conductivity estimate for the whole sample. Additional details are provided in the following section.

### 3. Statistical study of formation heterogeneity

The BHRS is a site with multi-scale heterogeneity across a spatial distribution of units, each of which exhibits spatial variability in hydraulic parameters (Barrash and Clemo, 2002; Barrash and Reboulet, 2004; Bradford et al., 2009). As shown in Fig. 2, five units are sub-horizontally distributed with boundaries or contacts that pinch and swell, as is common in braided stream deposits. Porosity logs were used to estimate porosity in 3551 locations across the site, and two statistical measures of the grain size distribution (i.e., matrix  $d_{10}$  and matrix fraction of the total grain size distribution) from about one thousand core samples from the aquifer were assigned to the five units at the BHRS. In this study we statistically characterize the porosity ( $n$ ), grain size distribution (GSD), and correlations within and between these data sets. We then construct a detailed model of hydraulic conductivity ( $K$ ) that is faithful to simulations of  $n$ , and GSD. This allows us to study flow and transport through the synthetic  $K$  fields, and explore the relative impact of  $n$  and GSD on solute transport.

Since the aquifer can be segregated into zones or units on the basis of large scale heterogeneities, this study focuses on statistical characterization of aquifer properties in individual units. We use Unit 3, a relatively homogeneous unit, as a conservative example since local scale heterogeneities are expected to have significantly more impact in other units at the site.

The modified Kozeny–Carman formula used to estimate hydraulic conductivity of the matrix,  $K_m$ , and the aquifer hydraulic conductivity,  $K$ , from porosity,  $n$ , and a characteristic grain size statistic  $d_{10}$  (the 10th percentile of grain sizes), is:

$$K_m = \frac{\rho g}{\mu} \cdot \frac{\phi^3 d_{10}^2}{180(1-\phi)^2} \quad \text{and} \quad K = K_m(n + V_m) \quad (1)$$

where  $\phi = \frac{n}{n + M(1-n)}$  is an effective porosity variable adjusted to represent the porosity for the matrix alone (i.e., excluding the fraction of framework cobble grains that effectively do not participate in the flow),  $\rho$  is fluid density,  $g$  is the gravitational acceleration,  $\mu$  is the fluid viscosity and  $M$  is the matrix volume fraction of the grain size distribution defined as the percentage of grain sizes, by weight, below approximately 10 mm (Smith, 1986; Jussel et al., 1994; Barrash and Reboulet, 2004). In the application of Eq. (1),  $d_{10}$  and  $f$  are based on measurements, and the other parameters are physical constants. To connect formula (1) with the discussion in the previous section, note that the matrix fraction  $M = V_m / (V_m + V_c) = V_m / (1 - n)$  thus  $M(1 - n) = V_m$ . Recall that the matrix conductivity  $K_m$  is multiplied by  $(n + V_m)$  to recover a conductivity estimate for the whole sample.

By taking base ten logarithms on both sides of Eq. (1),  $\log K$  can be expressed as a sum of  $\log d_{10}$  and an additional term that depends on  $n$  and  $M$  (which are measured) through the variable  $\phi$ . To simplify, we suppose that  $\log K$  is a simple linear function of  $n$ ,  $M$ , and  $\log d_{10}$ , plus some additional random error. Based on the Unit 3 borehole data, we develop a regression model:

$$\log K = -1.14 - 0.0228M + 8.28n + 2.02\log d_{10}. \quad (2)$$

The regression parameters are specific to this unit and site, and should not be taken as a universal model. Our motivation for considering a regression model is to understand the relative contribution of the three variables  $n$ ,  $M$ , and  $\log d_{10}$  to the resulting  $K$  field. This allows us to generate multiple realizations of stochastic porosity and hydraulic conductivity fields. Variations in  $n$ ,  $M$ , and  $\log d_{10}$  explain 98.9% of the variations in  $\log K$  for this regression model (i.e. the  $R$ -squared value is 98.9%). All regression coefficients are statistically significant with a  $P$ -value of  $<0.0005$ , indicating that all three variables contribute significant new information about  $\log K$ . This is confirmed with a sequential sum of squares analysis that indicates all three variables significantly inform the model, with the porosity being the most significant. The cross-correlations of the three input variables were also examined. There is a 0.270 correlation between  $M$  and  $d_{10}$  which is statistically significant with  $P < 0.0005$ , but there are no significant correlations between porosity ( $n$ ) and the grain size variables  $\log d_{10}$  and  $M$ . Correlations between the input variables can obfuscate the relative contributions of the input parameters (as measured in the sequential sum of squares) as well as the meaning of the regression coefficients. Since porosity is uncorrelated with the grain size distribution variables in this case, the meaning of the regression coefficient for  $n$  is unambiguous. In summary, Eq. (2) can be used to simulate the  $\log K$  field, once we simulate the three input variables using the appropriate probability distributions and correlation structure. Next, we examine each input variable by statistically characterizing the data from Unit 3.

### 4. Hydraulic conductivity simulation

We investigated the statistical properties of the three input variables in the regression model (Eq. (2)), and then developed a procedure for generating  $K$  fields that are statistically consistent with the Unit 3 borehole data. We began with the statistics of the grain size distribution. The variable  $M$  is the percentage of a core sample, by weight, that passes

through a 9.525 mm sieve. Hence the units are percent. The model for  $M$  is quite simple. Fig. 3 (right panel) shows that the data from Unit 3 are reasonably well described by a normal random variable with mean of 39% and standard deviation of 7.3%. A normal probability plot of  $M$  (not shown) also indicates a good fit, and the Anderson–Darling test for normality yields an associated  $P$ -value of 0.369, which provides additional justification for assuming a normal distribution. A spatial autocorrelation plot for  $M$  in Unit 3 (not shown) indicates that these values from the borehole are uncorrelated in the vertical direction.

The variable  $d_{10}$  represents the 10th percentile of the matrix grain size distribution in mm, estimated by curve fitting through the sieve data. Base ten logarithms were used to compute the input variable  $\log d_{10}$  for the  $K$  field simulation. The spatial autocorrelation function (not shown) indicates that the  $\log d_{10}$  data exhibit some spatial correlation. Fig. 3 (left panel) shows that  $\log d_{10}$  can be adequately modeled by a normal distribution (one outlier at  $-0.30$  was included in the pdf fitting procedure but is not shown on the histogram to avoid distorting the graph). Some additional comments on the normal fit appear at the end of this section. Hence our model for  $\log d_{10}$  is a correlated Gaussian random field with the same mean ( $m = -0.7376$ ) and standard deviation ( $s = 0.07$ ) as the Unit 3 data. Fig. 4 (left panel) shows an example of a simulated  $\log d_{10}$  random field for this unit. A standardized field  $Z$  (Gaussian with mean zero and standard deviation one) was rescaled using  $\log d_{10} = m + sZ$ . To enforce the  $\rho = 0.23$  correlation between  $M$  and  $\log d_{10}$  and to maintain the proper distribution of  $M$ , we then set  $M = 7.3 + 0.39(\rho Z + W) / (1 + \rho^2)$  where  $W$  is another independent Gaussian random field with the same correlation structure as  $Z$ . The resulting simulated  $M$  field (Fig. 4, right panel) is similar in appearance to the  $\log d_{10}$  random field shown in Fig. 4, left panel. Note that the correlation lengths of  $M$  and  $\log d_{10}$  are assumed to be the same, since both relate to the same grain size distribution.

As noted above, the porosity log data were measured at 0.06 m intervals and then averaged over the length of a given core sample to get the  $n$  data for a core sample interval. Fig. 5 (left panel) shows that the porosity data are skewed. Taking natural logarithms of the porosity data (Fig. 5, right panel) results in a distribution with a normal probability density

function (mean  $-1.744$ , standard deviation  $0.1221$ ,  $P = 0.474$ ), equivalent to fitting a lognormal distribution to the original data. The statistical hypothesis for the Anderson–Darling test states that the data fit a normal distribution. The large  $P$ -value indicates insufficient evidence to reject that hypothesis, showing that the normal fit is reasonable.

Next we examine spatial correlations in the porosity data. Since the porosity logs were taken at a finer resolution than the length of core samples, we use the log data to evaluate the correlation structure. Fig. 6 (left panel) shows the vertical spatial autocorrelation function for the  $\ln n$  data for Unit 3. The autocorrelation function indicates the signature of long range dependence (LRD), with correlation falling off slowly. Hence, we consider a model where serial correlation falls off like a power law function of spatial separation, sometimes called a fractal correlation model.

A standard way to check for LRD is to examine the power spectrum for power law growth near the origin. For LRD the power spectrum varies like frequency to the power  $-2d$  near zero, where  $d$  is the order of fractional integration. The Hurst index of self-similarity is related to the order of fractional integration by  $H = d + 1/2$ , see for example Benson et al. (2006). We checked for a power law spectrum by plotting natural logarithms of the periodogram versus Fourier frequency, and performed a linear regression (not shown), which yielded an estimate of  $d = 0.45$ . Next we subtracted the mean ( $1.768$ ) and fractionally differenced the data. Standard statistical tests indicate that the residuals (fractionally differenced, mean centered, natural logarithms of Unit 3 porosity log data) resemble a sequence of uncorrelated Gaussian random variables, validating the fractional model. Fig. 6 (right panel) also indicates that fractional differencing removed the serial correlation.

From the above analyses, we conclude that the natural logarithms of the Unit 3 porosity measurements in a vertical borehole are well described by fractional Brownian motion with Hurst parameter  $H = d + 1/2 = 0.95$ . This can be simulated using a standard spectral method with a power law filter, see Benson et al. (2006) for more details and examples. Once a standardized (mean zero and standard deviation one) Gaussian field is simulated, we multiply by  $0.1221$  and subtract  $1.744$  to match the  $\ln n$  borehole data, and we then apply the exp

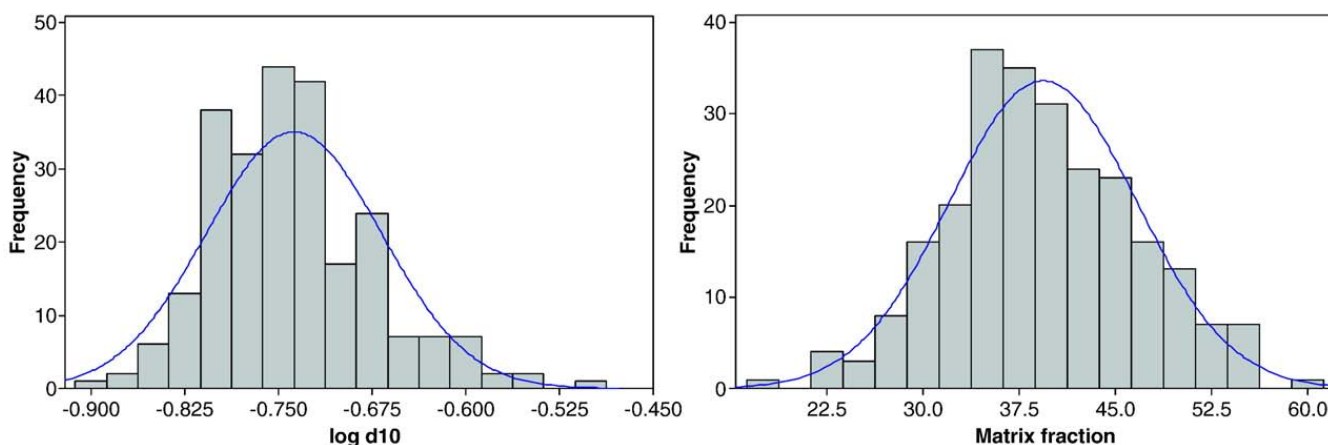


Fig. 3. Histogram and normal pdf for  $\log d_{10}$  (left) and matrix fraction  $M$  (right) in Unit 3.

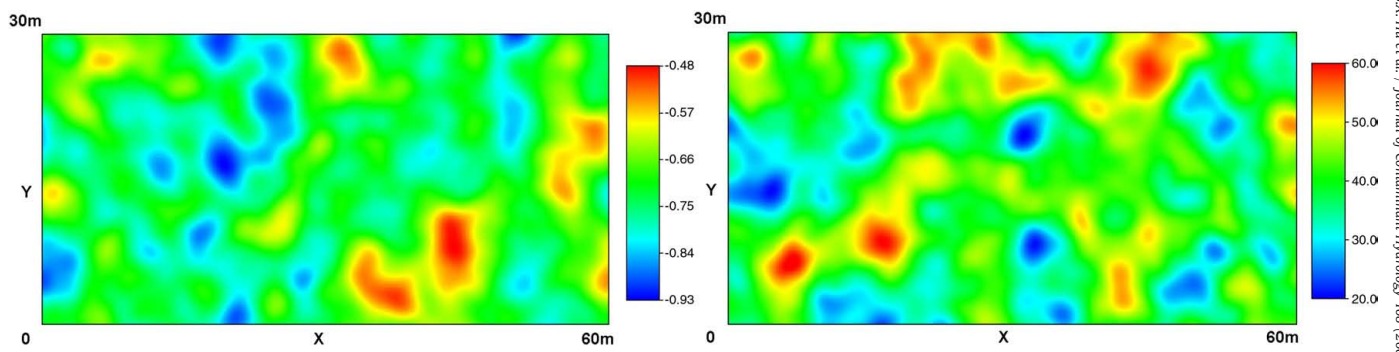


Fig. 4. Simulated fields of the grain size statistics  $\log d_{10}$  (left) and matrix fraction  $M$  (right).

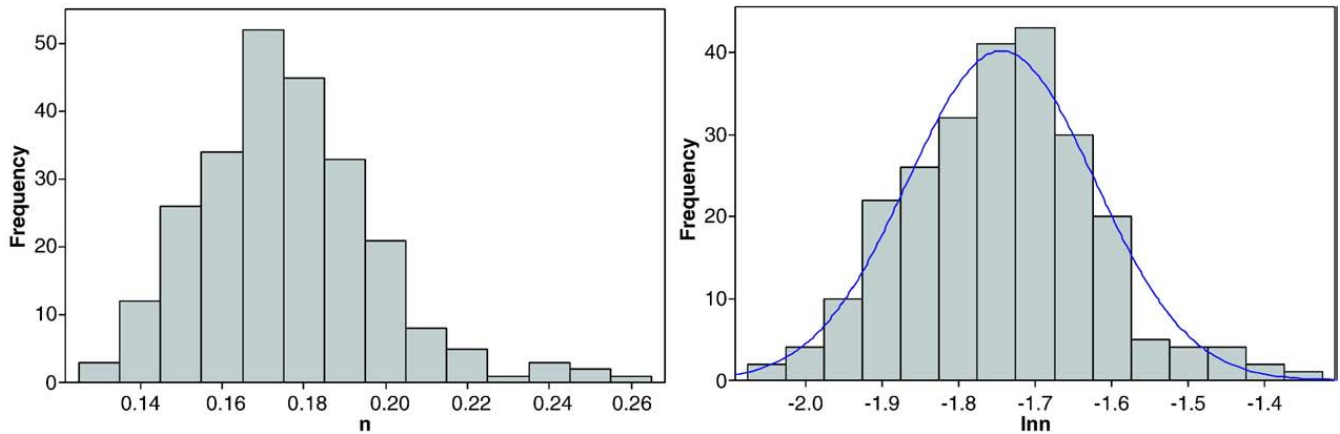


Fig. 5. Histograms of Unit 3 borehole porosity  $n$  (left) and  $\ln n$  with normal distribution curve superimposed (right).

function (inverse of the natural logarithm function) to get the simulated porosity field. Fig. 7 shows a typical fractal porosity field generated using this approach. The fractal field does not have a characteristic length (correlation length), and observable features (e.g., regions of high or low porosity) tend to be reproduced at every scale. Fractal models, and related nonlocal models, have significant implications for transport (Wheatcraft and Tyler, 1998; Benson et al., 2000; Cushman and Ginn, 2000; Neuman and Tartakovsky, 2008), but a full discussion is beyond the scope of this paper.

In summary, based on Eq. (2), we can simulate a representative  $K$  field as follows: We generate  $\log d_{10}$  as an exponentially correlated Gaussian random field with the same mean  $m = -0.7376$  and standard deviation  $s = 0.07$  as the borehole data. Next, we generate  $M$  as a linear combination of the  $\log d_{10}$  field and another independent Gaussian field, to preserve the correlation between these two grain size distribution descriptors, and adjust to the mean (39%) and standard deviation (7.3%) of the borehole data. Fractional Brownian motion provides a reasonable model for the natural logarithms of the porosity log data. Essentially, we generate uncorrelated standard normal random fields and fractionally integrate them with order  $d = 0.45$  (a specific linear filter) to get the appropriate correlation structure, adjust to mean  $-1.744$  and standard deviation

0.1221 to match the log-transformed borehole data, and then apply the exp function to get the simulated porosity logs.

Finally, we substitute the three input variables at each spatial coordinate into the linear regression Eq. (2) to get the log  $K$  field. In preparation for the plume simulations discussed below, we generated two-dimensional log  $K$  fields oriented in the flow direction and the transverse direction ( $x$ - $y$  plane). Lacking any explicit information on the spatial correlation structure in the  $x$ - $y$  plane, we assume a reasonable 10 m correlation length for the log  $d_{10}$  and  $M$  fields based on relative magnitudes for vertical and horizontal correlation lengths in similar natural aquifers (e.g. Table 1 in Jussel et al., 1994; Anderson, 1997). We account for the stronger correlation pattern expected in the  $x$ - $y$  plane by using a fractional Brownian field for log porosity (a nonstationary random field whose increments form a fractional Gaussian noise). Fig. 7 shows a typical porosity field generated this way. Fig. 8a and b shows the log  $K$  fields that result from combining the log  $d_{10}$  and  $M$  fields from Fig. 4 with a constant porosity and the stochastic porosity field in Fig. 7, respectively, via the regression Eq. (2). From Fig. 8a and b, one can see the influence of the heterogeneous porosity field on the generated hydraulic conductivity field. In general, the log  $K$  field inherits much of its structure from the porosity field, since porosity exhibits spatial LRD. One interpretation is that the porosity field codes the large scale

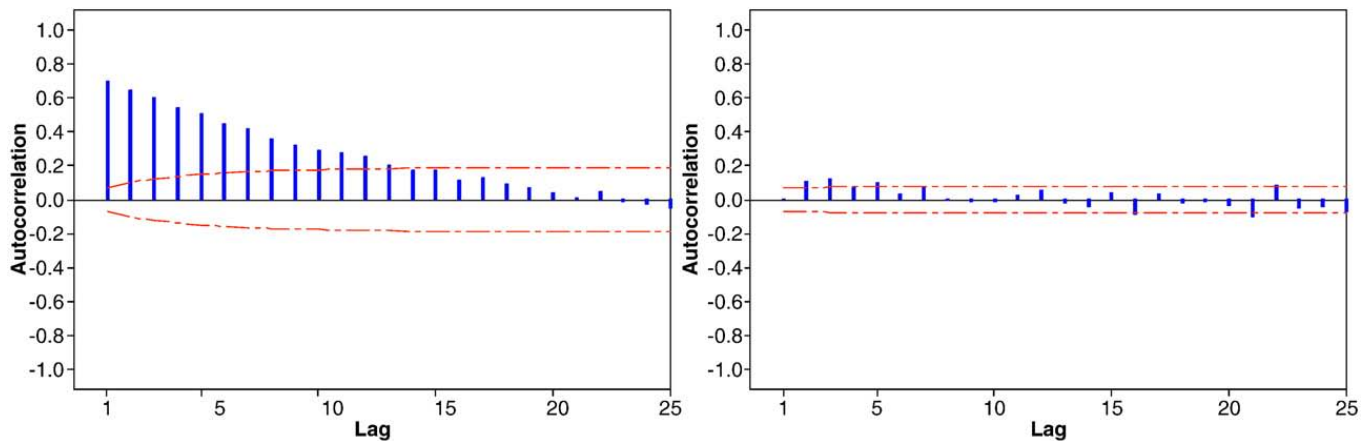


Fig. 6. Spatial autocorrelation function for  $\ln n$  (left) showing long range dependence. Residuals after fractional differencing (right) showing that the dependence has been removed. One lag equals 0.06 m, the spatial separation of the porosity log data.

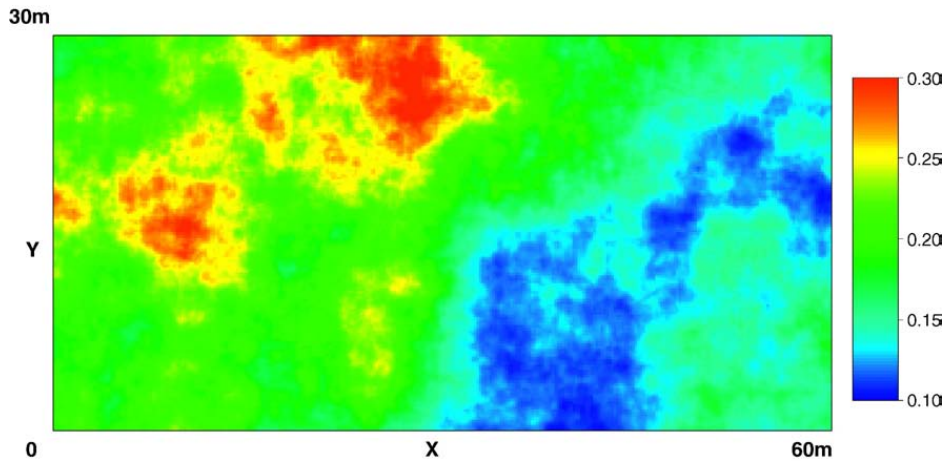


Fig. 7. Simulated fractal porosity field.

structure of the aquifer, while the grain size distribution codes the small scale roughness. In this unit of the BHRS, porosity appears to be the most important parameter to characterize for accurate estimation of hydraulic conductivity. We recognize that the  $K$  data used in this study were computed from the Kozeny–Carman formula (1) and, therefore, the correlation between  $K$  and the

three input variables ( $n$ ,  $\log d_{10}$  and  $M$ ) in the model (2) may be different in practice. Further research to develop high spatial resolution co-located measurements of  $K$ , porosity, and the grain size distribution is in progress to clarify this issue. We also note that the  $\log d_{10}$  distribution shows a deviation from normal ( $P < 0.05$ ) that could impart a heavier tail to the largest  $K$  values.

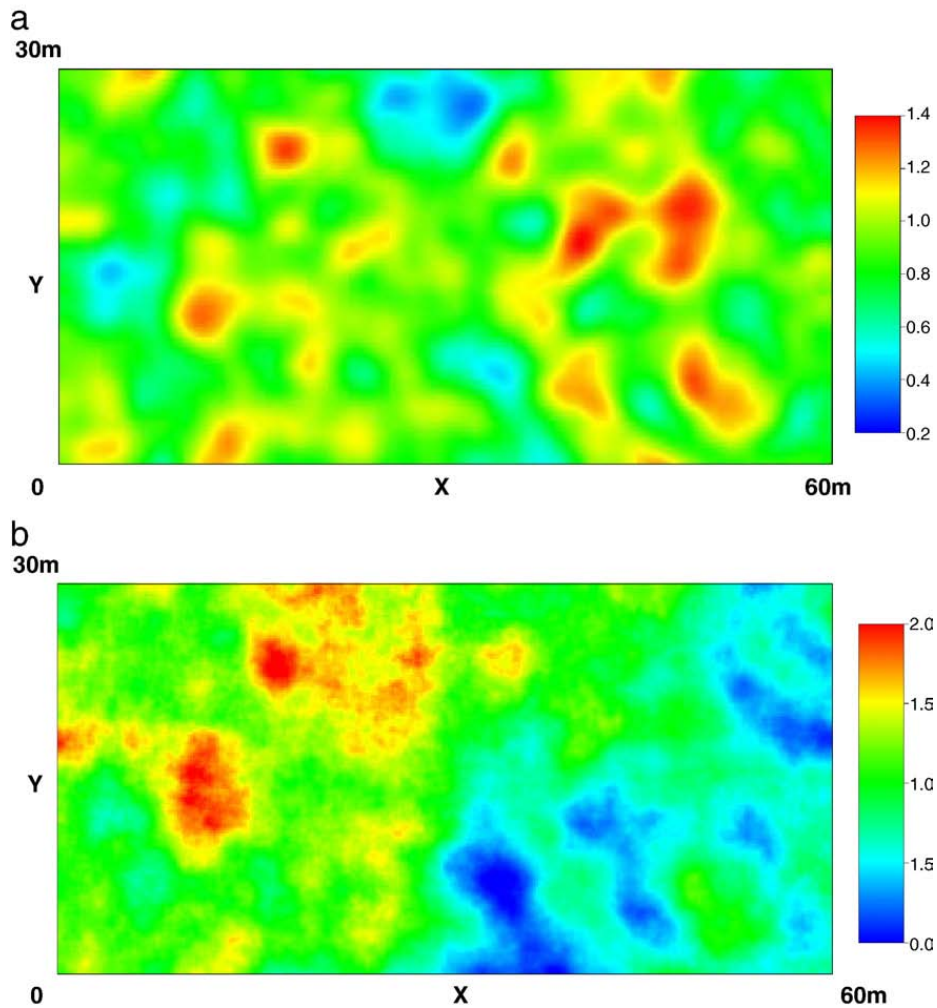


Fig. 8. (a) Simulated fractal log  $K$  field (log m/day) combining Fig. 4 and constant porosity field via model Eq. (2) used in case B. (b) Simulated fractal log  $K$  field (log m/day) combining Figs. 4 and 7 via model Eq. (2) used in case C.



### 5. Effects of hydraulic conductivity and porosity heterogeneity on flow and transport

Based on the generated porosity and conductivity fields, we investigate the effects of heterogeneous porosity fields on solute transport. A synthetic two-dimensional domain of dimensions 60 m (in  $x$ -direction) by 30 m (in  $y$ -direction) is used. We assume a no-flow boundary condition for the lateral (top and bottom) boundaries and constant heads at the inflow and outflow (left and right side) boundaries, with a mean gradient of 0.001, similar to the natural gradient at the BHRS (Barrash et al., 2002). The solute source is instantly released close to the left side boundary with an initial concentration of 100 mg/L. MODFLOW (Harbaugh, 2005) is used to simulate groundwater flow through a uniform grid with  $0.2\text{ m} \times 0.2\text{ m}$  cells, and a numerical particle tracking method from MT3DMS (Zheng and Wang, 1999) is used to simulate solute transport. Longitudinal and transverse dispersivity values are assumed to be 0.1 m and 0.01 m, respectively, based on modeling of

conservative transport behavior at the BHRS (Leven et al., 2002; Nelson, 2007).

To investigate the effect of porosity heterogeneity on solute transport, three cases with different spatial distributions of porosity and conductivity are considered. In case A, conductivity and porosity are both held constant with the mean values of the random fields. In case B, the porosity is still constant, but conductivity is variable due to the variations in  $\log d_{10}$  and  $M$ . In case C, porosity is assumed to be a random variable, so the variability of conductivity is due to variations in all three of its components. To develop statistics related to the transport behavior for the three cases, we run numerical transport experiments through 100 equally-likely realizations of the  $n$  and  $K$  fields based on the geostatistical study of the spatial parameters discussed earlier.

One realization of the concentration distributions at time 450 days and breakthrough curves through the right boundary are shown in Fig. 9 for the three cases. The plume distribution in Fig. 9a has a typical plume shape for a homogeneous medium

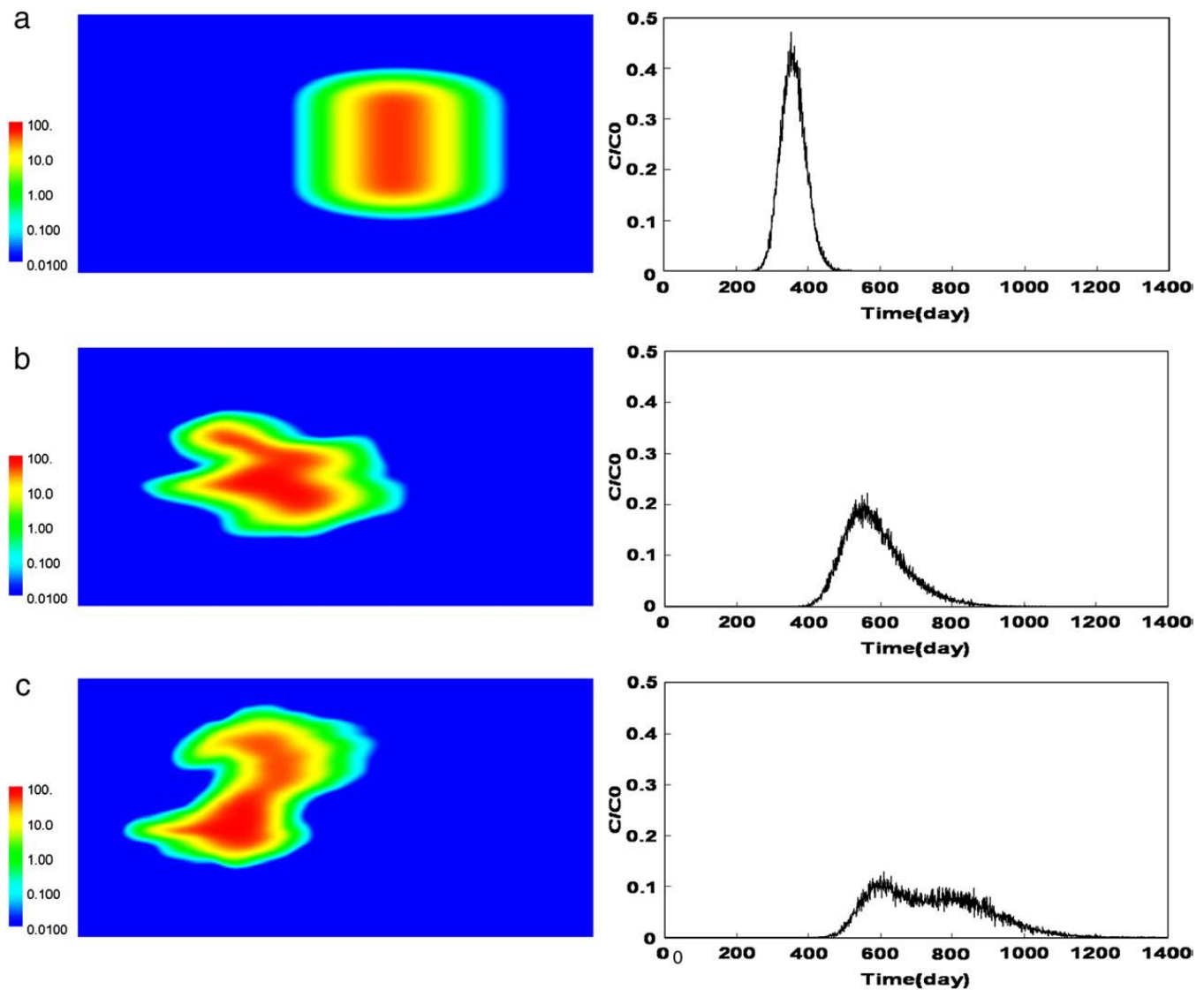


**Fig. 9.** Concentration distributions at  $T=450$  days and solute breakthrough curves through the right boundary for the three cases based on the porosity and conductivity fields in Figs. 7 and 8: (a) constant hydraulic conductivity and porosity, (b) stochastic conductivity and constant porosity, (c) stochastic conductivity and porosity.

with high concentrations near the plume center and gradual decrease toward the inflow and outflow boundaries, and the breakthrough curve has a typical Gaussian-type distribution. The plume in Fig. 9b is irregular and clearly stretched by velocity variations. The breakthrough curve shows a nonsymmetric distribution, with a wider range and lower peak relative to case A. For the case with variable conductivity and porosity (Fig. 9c), the plume is very irregular and strongly stretched. Two high-concentration centers appear due to preferential flow patterns, which is clearly one mechanism for multiple-peaked tracer concentration histories at monitoring wells. The breakthrough is thus very irregular, with two peaks and a strongly negative-skewed distribution. Porosity variability in this example clearly increases the plume spreading, makes the curve more negatively skewed, and causes two peaks in the breakthrough curve.

For each of the 100 realizations of conductivity or/and porosity fields, we calculate the solute breakthrough curve

through the right boundary of the study domain for the three cases described above. Based on the results of 100 realizations for each case, we calculate the mean breakthrough curve, and the standard deviation from the mean. The mean breakthrough curves over the 100 realizations for the three cases are shown in Fig. 10a. The breakthrough curve for constant  $K$  and porosity (case A) has a normal distribution with a narrow spread. Adding spatial variability of hydraulic conductivity (case B) distorts the mean breakthrough curve such that it no longer has a normal distribution. In comparison with the homogeneous case, the breakthrough curve has been significantly extended and the peak concentration significantly decreased. The mean breakthrough curve is negatively skewed, which is similar to the single realization result shown in Fig. 9b. For case C with spatially variable conductivity and porosity, the mean arrival time is significantly delayed, and the peak concentration is significantly decreased.

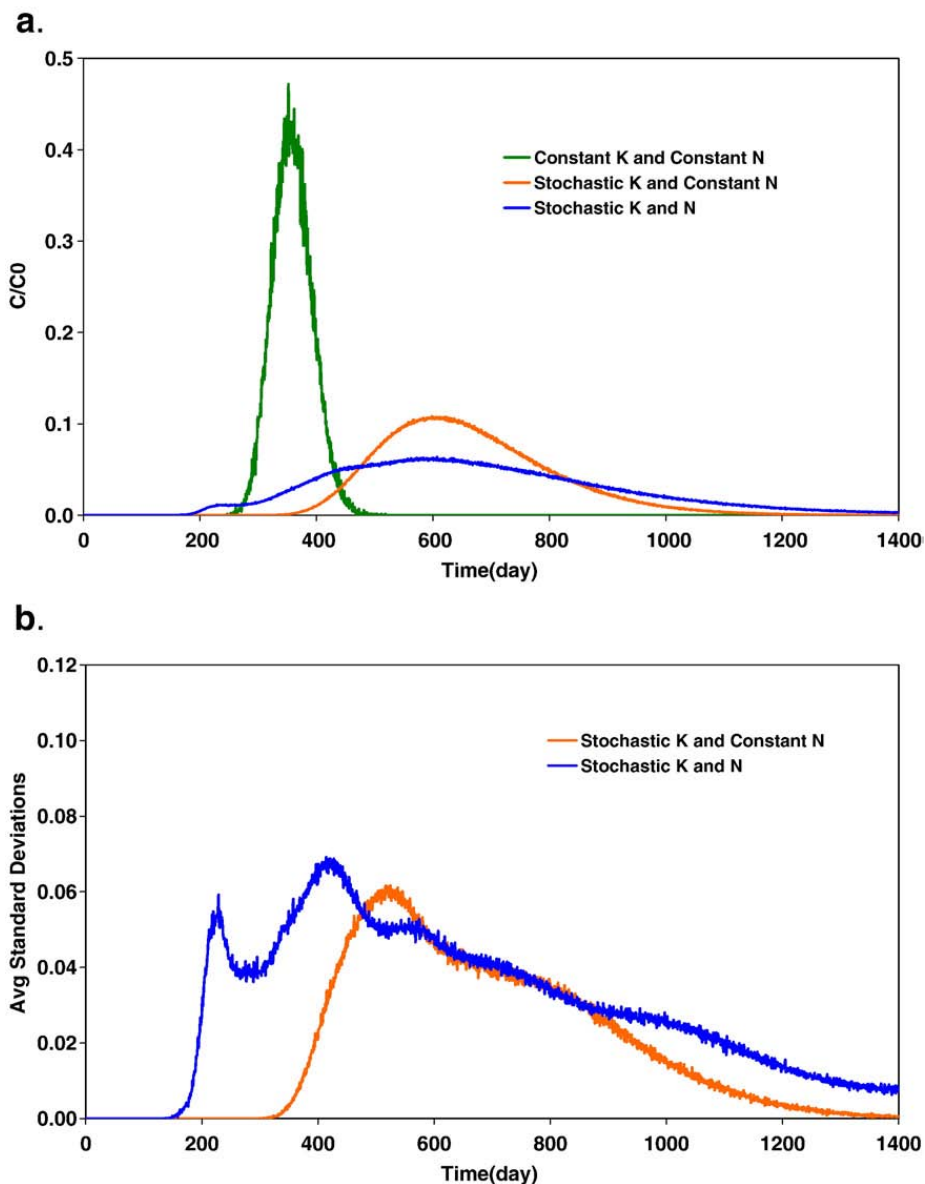


Fig. 10. Mean and standard deviation of breakthrough curves for the three cases. a. Mean breakthrough curves. b. Averaged standard deviations of breakthrough curves.

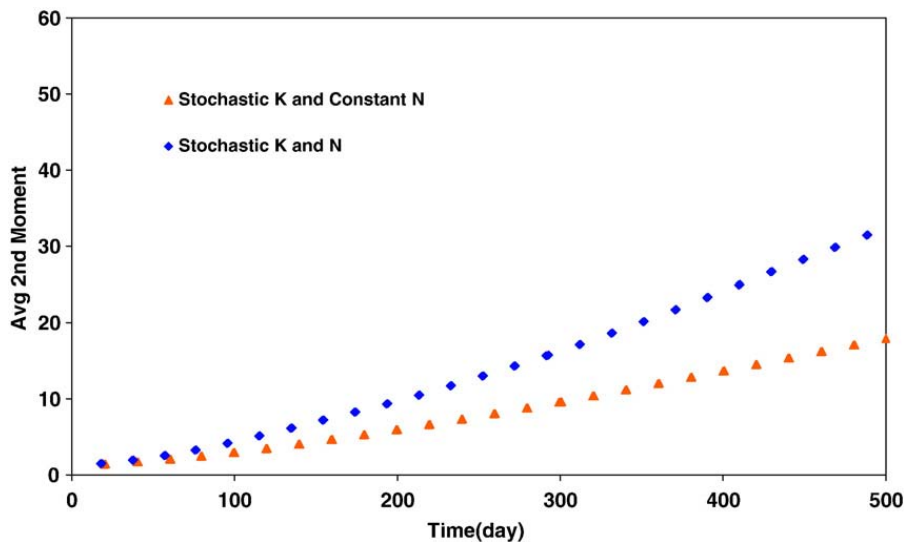


Fig. 11. Spatial second longitudinal moments for cases B and C.

In comparison with the single realization result shown in Fig. 9c, only one peak exists as the second is removed through the averaging calculation over the 100 realizations.

The standard deviations from the mean breakthrough curves for cases B and C are shown in Fig. 10b. The shapes and characteristics of the standard deviation curves for cases B and C are similar to the mean curves. However, for case C, the two-peaked distributions are more obvious in the standard deviation curve.

To track and compare the spreading of the solute plumes, we calculate the second spatial moments for cases B and C, as shown in Fig. 11. Adding heterogeneity to the porosity field significantly increases the second longitudinal moment, which is consistent with the breakthrough curve results.

## 6. Summary and conclusions

In this study, based on the porosity measurements and particle size analysis of borehole samples from the Boise Hydrogeophysical Research Site (BHRS), we evaluate the heterogeneous porosity and grain size characteristics of the geological formation. Porosity data collected from the wells are used to study the geostatistical structure in Unit 3. This relatively homogeneous unit was chosen as the basis for generating our aquifer realizations with the idea that this would be a good threshold test of the significance of including the spatial variability of porosity in solute transport models.

We estimated the spatial distribution of hydraulic conductivity using a regression-based relationship linked to geostatistical analysis of porosity and particle size data obtained from borehole measurements from the BHRS. By examining a histogram and probability plot of porosity and particle size data for Unit 3, along with autocorrelation functions for porosity and particle size distributions, we built a statistical model for the two quantities. We also investigated the correlation among porosity, the tenth percentile of the particle size distribution, matrix fraction, and hydraulic conductivity. Based on the stochastic hydraulic conductivity fields, we used MODFLOW and a particle tracking method in MT3DMS to study the effects of porosity and hydraulic conductivity heterogeneities on solute transport.

Based on this study, we make the following conclusions:

1. This study characterizes heterogeneity in 2D within one unit, and examines the effect of heterogeneity in both porosity and derived hydraulic conductivity fields on solute transport. Plausible hydraulic conductivity realizations can be obtained through geostatistical characterization using data that are relatively simple to collect: particle size data and borehole neutron (porosity) log data.
2. The porosity distribution in the study unit fits a lognormal model with a fractal correlation structure.
3. Porosity heterogeneity is important to characterize and include in groundwater flow and transport models as it can enhance irregular plume distributions, delay and spread solute breakthrough curves, and increase plume second moments. Randomness in porosity fields also appears to cause breakthrough curves to be more skewed and cause multiple peaks.
4. The presence of significant effects due to inclusion of porosity heterogeneity in 2D realizations of a mildly heterogeneous system indicates the need to better understand the relationship between porosity and conductivity distributions and resulting influence on flow and transport under a broad range of dimensionality, heterogeneity, and natural and forced gradient conditions.

## Acknowledgements

Thanks to Professor Hans-Peter Scheffler, University of Siegen, Germany, for allowing us to use his MATLAB code for generating fractal random fields. Support for Dr. Barrash provided by EPA grant X-96004601-0. We also gratefully acknowledge the comments of three anonymous reviewers, which significantly improved the presentation.

## References

- Anderson, M.P., 1997. Characterization of geological heterogeneity. In: Dagan, G., Neuman, S.P. (Eds.), *Subsurface Flow and Transport: a Stochastic Approach*. International Hydrologic Series. Cambridge University Press, Cambridge, UK, pp. 23–43.

- Archie, G.E., 1950. Introduction to petrophysics of reservoir rocks. *Bulletin of the American Association of Petroleum Geologists* 34 (5), 943–961.
- Atkins, J.E., McBride, E.F., 1992. Porosity and packing of Holocene river, dune, and beach sands. *AAPG Bulletin* 76 (3), 339–355.
- Barrash, W., Clemo, T., 2002. Hierarchical geostatistics and multifacies systems: Boise Hydrogeophysical Research Site, Boise, Idaho. *Water Resources Research* 38 (10), 1196. doi:10.1029/2002WR001436.
- Barrash, W., Reboulet, E.C., 2004. Significance of porosity for stratigraphy and textural composition in subsurface coarse fluvial deposits, Boise Hydrogeophysical Research Site. *Geological Society of America Bulletin* 116 (9/10). doi:10.1130/B25370.1.
- Barrash, W., Clemo, T., Knoll, M.D., 1999. Boise Hydrogeophysical Research Site (BHRS): Objectives, design, initial geostatistical results. *Proceedings of SAGEEP99*, pp. 389–398. March 14–18, 1999, Oakland, CA.
- Barrash, W., Clemo, T., Hyndman, D.W., Reboulet, E., Hausrath, E., 2002. Tracer/Time-Lapse Radar Imaging Test; Design, Operation, and Preliminary Results: Report to EPA for Grant X-970085-01-0 and to the U.S. Army Research Office for Grant DAAH04-96-1-0318, Center for Geophysical Investigation of the Shallow Subsurface Technical Report BSU CGISS 02-03. Boise State University, Boise, ID. 120 p.
- Benson, D.A., Wheatcraft, S.W., Meerschaert, M.M., 2000. Application of a fractional advection–dispersion equation. *Water Resources Research* 36 (6), 1403–1412.
- Benson, D.A., Meerschaert, M.M., Baeumer, B., Scheffer, H.P., 2006. Aquifer operator scaling and the effect on solute mixing and dispersion. *Water Resources Research* 42 (1).
- Bradford, J.H., Clement, W.P., Barrash, W., 2009. Estimating porosity with ground-penetrating radar reflection tomography: a controlled 3D experiment at the Boise Hydrogeophysical Research Site. *Water Resources Research* 45, W00D26. doi:10.1029/2008WR006960.
- Charbeneau, R.J., 2000. *Groundwater Hydraulics and Pollutant Transport*. Prentice Hall, Upper Saddle River, NJ, p. 593.
- Clarke, R.H., 1979. Reservoir properties of conglomerates and conglomeratic sandstones. *American Association of Petroleum Geologists Bulletin* 63 (5), 799–809.
- Clement, W.P., Knoll, M.D., Liberty, L.M., Donaldson, P.R., Michaels, P.M., Barrash, W., Pelton, J.R., 1999. Geophysical surveys across the Boise Hydrogeophysical Research Site to determine geophysical parameters of a shallow alluvial aquifer. *Proceedings of the Symposium on the Application of Geophysics to Engineering and Environmental Problems*, pp. 399–408. March 14–18, 1999, Oakland, CA.
- Cushman, J.H., 1997. *The Physics of Fluids in Hierarchical Porous Media: Angstroms to Miles*. Kluwer Academic.
- Cushman, J.H., Ginn, T.R., 2000. Fractional advection dispersion equation: a classical mass balance with convolution-Fickian flux. *Water Resources Research* 36 (12), 3763–3766.
- Dagan, G., 1989. *Flow and Transport in Porous Formations*. Springer-Verlag, Berlin.
- Fraser, H.J., 1935. Experimental study of the porosity and permeability of clastic sediments. *Journal of Geology* 43 (8), 910–1010 pt. 1.
- Freeze, R.A., Cherry, J.A., 1979. *Groundwater*. Prentice Hall, Upper Saddle River, NJ. 604 p.
- Gelhar, L.W., 1993. *Stochastic Subsurface Hydrology*. Prentice-Hall, Englewood Cliffs, N. J.
- Gelhar, L.W., Welty, C., Rehfeldt, K.R., 1992. A critical review of data on field-scale dispersion in aquifers. *Water Resources Research* 28 (7), 1955–1974.
- Guen, O., Molz, F.J., Melville, J.G., El Diddy, S., Boman, G.K., 1992. Three-dimensional modeling of a two-well tracer test. *Ground Water* 30 (6), 945–957.
- Harbaugh, A.W., 2005. MODFLOW-2005, the U.S. Geological Survey Modular Ground-water Model – the Ground-Water Flow Process: U.S. Geological Survey Techniques and Methods 6-A16.
- Hassan, A.E., 2001. Water flow and solute mass flux in heterogeneous porous formations with spatially random porosity. *Journal of Hydrology* 242, 1–25.
- Hassan, A.E., Cushman, J.H., Delleur, J.W., 1998. Significance of porosity variability to transport in heterogeneous porous media. *Water Resources Research* 34 (9), 2249–2259.
- Hearst, J.R., Nelson, P.H., 1985. *Well logging for physical properties*. McGraw-Hill, New York. 571 p.
- Heinz, J., Kleinedam, S., Teutsch, G., Aigner, T., 2003. Heterogeneity patterns of Quaternary glaciofluvial gravel bodies (SW-Germany): application to hydrogeology. *Sedimentary Geology* 158, 1–23. doi:10.1016/S0037-0738(02)00239-7.
- Hughes, C.E., 2005. Comparison of empirical relationships for hydraulic conductivity using grain size distribution, packing, and porosity information from the Boise Hydrogeophysical Research Site, Boise, Idaho: M.S. Thesis, Boise State University, Boise, ID. 123 p.
- Hyndman, D.W., Dybas, M.J., Forney, L., Heine, R., Mayotte, T., Phanikumar, M.S., Tatara, G., Tiedje, J., Voice, T., Wallace, R., Wiggert, D., Zhao, X., Criddle, C.S., 2000. Hydraulic characterization and design of a full-scale biocurtain. *Ground Water* 38 (3), 462–474.
- Jussel, P., Stauffer, F., Dracos, T., 1994. Transport modeling in heterogeneous aquifers: 1. Statistical description and numerical generation. *Water Resources Research* 30 (6), 1803–1817.
- Kapoor, V., Gelhar, L.W., 1994. Transport in three-dimensionally heterogeneous aquifers 2. Predictions and observations of concentration fluctuations. *Water Resources Research* 30 (6), 1789–1801.
- Keys, W.S., 1990. *Borehole Geophysics Applied to Ground-water Investigations: U.S. Geological Survey Techniques of Water-Resources Investigations, Book 2, Chapter E-2*. 149 p.
- Lahm, T.D., Bair, E.S., Schwartz, F.W., 1995. The use of stochastic simulations and geophysical logs to characterize spatial heterogeneity in hydrogeologic parameters. *Mathematical Geology* 27 (2), 259–278.
- Leven, C., Barrash, W., Hyndman, D.W., Johnson, T.C., 2002. Modeling a combined tracer and time-lapse radar imaging test in the heterogeneous fluvial aquifer at the Boise Hydrogeophysical Research Site (abs.). *EOS* 83 (47), F487.
- Mackay, D.M., Freyberg, D.L., Roberts, P.V., Cherry, J.A., 1986. A natural gradient experiment on solute transport in a sand aquifer 1. Approach and overview of plume movement. *Water Resources Research* 22 (13), 2017–2029.
- Mas-Pla, J., Yeh, T.-C.J., McCarthy, J.F., Williams, T.M., 1992. A forced gradient tracer experiment in a coastal sandy aquifer, Georgetown site, South Carolina. *Ground Water* 30 (6), 958–964.
- Meerschaert, M.M., Kozubowski, T.J., Molz, F.J., 2006. Fractional Laplace model for hydraulic conductivity. *Geophysical Research Letters* 31 (8), 1–4. doi:10.1029/2003GL019320.
- Molz, F.J., Rajaram, H., Lu, S., 2004. Stochastic fractal-based models of heterogeneity in subsurface hydrology: origins, applications, limitations, and future research questions. *Review of Geophysics* 42, RG1002. doi:10.1029/2003RG10026.
- Nelson, G.K., 2007. Deterministic modeling of bromide tracer transport during the tracer/time-lapse radar imaging test at the Boise Hydrogeophysical Research Site, August 2001: M.S. Thesis, Boise State University, Boise, ID. 172 p.
- Nelson, P.H., 1994. Permeability–porosity relationships in sedimentary rocks. *Log Analyst* 35 (3), 38–62.
- Neuman, S.P., Riva, M., Guadagnini, A., 2008. On the geostatistical characterization of hierarchical media. *Water Resources Research* 44, W02403. doi:10.1029/2007WR006228.
- Neuman, S.P., Tartakovsky, D.M., 2008. Perspective on theories of non-Fickian transport in heterogeneous media. *Advances in Water Resources* 32 (5), 670–680.
- Panda, M.N., Lake, L.W., 1994. Estimation of single-phase permeability from parameters of particle-size distribution. *American Association of Petroleum Geologists Bulletin* 78 (7), 1028–1039.
- Pettyjohn, F., Potter, P., Siever, R., 1973. *Sand and Sandstone*. Springer-Verlag, New York. 618 pp.
- Phanikumar, M.S., Hyndman, D.W., Zhao, X., Dybas, M.J., 2005. A three-dimensional model of microbial transport and biodegradation at the Schoolcraft, Michigan, site. *Water Resources Research* 41, W05011. doi:10.1029/2004WR003376.
- Pryor, W.A., 1973. Permeability–porosity patterns and variations in some Holocene sand bodies. *American Association of Petroleum Geologists Bulletin* 57 (1), 162–189.
- Reboulet, E.C., Barrash, W., 2003. Core, Grain-size, and Porosity Data from the Boise Hydrogeophysical Research Site: Center for Geophysical Investigation of the Shallow Subsurface Technical Report BSU CGISS 03-02. Boise State University, Boise, ID. 87 p.
- Rider, M.H., 1996. *The Geological Interpretation of Well Logs*, 2nd ed. Gulf Publishing Co., Houston. 280 pp.
- Riva, M., Guadagnini, L., Guadagnini, A., Ptak, T., Martac, E., 2006. Probabilistic study of well capture zones distribution at the Luswiesen field site. *Journal of Contaminant Hydrology* 88, 92–118.
- Riva, M., Guadagnini, A., Fernandez-Garcia, D., Sanchez-Vila, X., Ptak, T., 2008. Relative importance of geostatistical and transport models in describing heavily tailed breakthrough curves at the Laiswiesen site. *Journal of Contaminant Hydrology* 101, 1–12.
- Rubin, Y., 2003. *Applied Stochastic Hydrogeology*. Oxford Univ. Press.
- Salamon, P., Fernandez-Garcia, D., Gomez-Hernandez, J.J., 2007. Modeling tracer transport at the MADE site: the importance of heterogeneity. *Water Resources Research* 43, W08404. doi:10.1029/2006WR005522.
- Smith, G.A., 1986. Coarse-grained nonmarine volcanoclastic sediment: terminology and depositional processes. *Geological Society of America Bulletin* 97, 1–10.
- Wheatcraft, S., Tyler, S., 1998. An explanation of scale-dependent dispersivity in heterogeneous aquifers using concepts of fractal geometry. *Water Resources Research* 24 (4), 566–578.
- Zhang, D., 2002. *Stochastic Methods for Flow in Porous Media: Coping with Uncertainties*. Academic Press, San Diego, CA. 350 pp.
- Zheng, C., Wang, P., MT3DMS, 1999. A modular three-dimensional multi-species transport model for simulation of advection, dispersion and chemical reactions of contaminants in groundwater systems: documentation and user's guide. Technical Report, U.S. Army Engineer Research and Development Center Contract Report SERDP-99-1, Vicksburg, MS, 1999.